Letter

# Multistep SlipChip for the generation of serial dilution nanoliter arrays and HBV viral load quantification by digital LAMP

Mengchao Yu, Xiaoying Chen, Haijun Qu, Liang Ma, Lei Xu, Weiyuan Lv, Hua Wang, Rustem F. Ismagilov, Min Li, and Feng Shen

*Anal. Chem.*, **Just Accepted Manuscript** • Publication Date (Web): 22 May 2019

# Multistep SlipChip for the generation of serial dilution nanoliter arrays and HBV viral load quantification by digital LAMP

Mengchao Yu[a], Xiaoying Chen[b], Haijun Qu[a], Liang Ma[c†], Lei Xu[a], Weiyuan Lv[a], Hua Wang[b], Rustem F. Ismagilov[d,e], Min Li[b,f]* and Feng Shen[a]*

a. School of Biomedical Engineering, Shanghai Jiao Tong University, Shanghai, 200030, China.
b. Department of Laboratory Medicine, Renji Hospital, School of Medicine, Shanghai Jiao Tong University, Shanghai 200127, China.
c. Department of Chemistry and Institute for Biophysical Dynamics, The University of Chicago, 929 East 57th Street, Chicago, Illinois 60637, United States.
d. Division of Chemistry & Chemical Engineering, California Institute of Technology, 1200 East California Boulevard, Mail Code 210-41, Pasadena, California, 91125, United State.
e. Division of Biology & Biological Engineering, California Institute of Technology, 1200 East California Boulevard, Mail Code 210-41, Pasadena, California 91125 United States.
f. China State Key Laboratory of Microbial Resources, Institute of Microbiology, Chinese Academy of Sciences, Beijing, 100080, China.

**ABSTRACT:** Serial dilution is a commonly used technique that generates a low-concentration working sample from a high-concentration stock solution and is used to set up screening conditions over a large dynamic range for biological study, optimization of reaction conditions, drug screening, etc. Creating an array of serial dilutions usually requires cumbersome manual pipetting steps or a robotic liquid handling system. Moreover, it is very challenging to set up an array of serial dilutions in nanoliter volumes in miniaturized assays. Here, a multistep SlipChip microfluidic device is presented for generating serial dilution nanoliter arrays in high throughput with a series of simple sliding motions. The dilution ratio can be precisely predetermined by the volumes of mother microwells and daughter microwells, and this paper demonstrates devices designed to have dilution ratios of 1:1, 1:2, and 1:4. Furthermore, an eight-step serial dilution SlipChip with a dilution ratio of 1:4 is applied for digital LAMP across a large dynamic range and tested for hepatitis B viral load quantification with clinical samples. With 64 wells of each dilution and fewer than 600 wells in total, the serial dilution SlipChip can achieve a theoretical quantification dynamic range of 7 orders of magnitude.

This paper describes a serial dilution SlipChip (sd-SlipChip) for generating nanoliter arrays with a wide range of stepwise concentrations for biochemical analysis. Serial dilution is a common laboratory practice used to generate solutions with relatively low concentrations from high-concentration samples. It is also widely used to set up an array, such as arrays in 96- or 384-well plate format, for screening conditions or performing quantification over a large dynamic range.[1–4] In practice, serial dilution is usually performed with tedious multiple manual pipetting steps or an often expensive robotic liquid handling system. With these traditional fluid handling methods, it is nontrivial to precisely control fluidic volumes at low microliter volumes, especially the nanoliter range, during each fluidic transferring step.

Microfluidics has been demonstrated as an excellent method to control and manipulate small volumes,[5] and several microfluidic systems were demonstrated to generate a chemical gradient[6–11] but not partitions in serial dilution. Valve-driven microfluidic strategies were also applied to control mixing and create serial dilution compartments;[12,13] however, these methods rely on accurate pneumatic control to operate the valves. A serial dilution microfluidic network consisting of microchannels was demonstrated to generate arbitrary concentration profiles,[14] and a centrifugal microfluidic device was also able to produce partitions with serial diluted concentrations.[15] However, it is challenging for these approaches to create nanoliter arrays via serial dilution.

In this paper, the sd-SlipChip utilized simple multistep sliding motions to produce serial dilution nanoliter arrays with precise dilution ratios, and we also applied this SlipChip device with both x and y direction movement to achieve designed fluidic handling goals. Furthermore, we demonstrated the sd-SlipChip quantifying a target nucleic acid over a large dynamic range by serial dilution digital loop-mediated isothermal amplification (LAMP) and tested it with HBV viral load quantification with sixteen clinical samples.

Digital nucleic acid amplification (NAA) methods, such as digital PCR and digital isothermal amplification, are considered accurate for nucleic acid quantification.[16,17] These methods have been applied for a variety of applications, including detection of fetal DNA in maternal blood,[18] quantification of viral load,[19] analysis of DNA methylation[20] and study of circulating tumor DNA (ctDNA) in cancer patients.[21] In general, digital NAA can be performed using droplet-based methods[16,22–25] or chamber-based devices,[26–33] which can divide

a solution containing target nucleic acids into a large number of nanoliter or subnanoliter reaction compartments. After amplification, the partitions can be determined as "positive" or "negative" based on the fluorescence intensity, and the initial concentration of target nucleic acids can be calculated based on Poisson statistics.[34]

To quantify target molecules over a large dynamic range, such as for the analysis of viral load,[35–37] the dynamic range of traditional digital NAA is generally limited by droplet volume and the total number of partitions. However, the sd-SlipChip can achieve a large dynamic range with significantly fewer partitions than other methods. For instance, to reach a theoretical dynamic range of 7 orders of magnitude, traditional digital NAA requires millions of 1 nL droplets, while the sd-SlipChip requires fewer than 600 microwells. This makes the sd-SlipChip particularly interesting for the quantification of viral load over a large dynamic range. In this paper, we demonstrated quantification of hepatitis B viral load with digital LAMP with large dynamic range in an sd-SlipChip. Hepatitis B virus (HBV) can cause life-threatening liver infections that may result in cirrhosis and liver cancer. Quantitative measurement of HBV load is crucial to understand patient status and to provide proper treatment. The current real-time qPCR method is routinely used in central hospitals, but due to the requirement of a designated space, skilled personnel and the cost of instruments, it is unlikely for these methods to be widely practiced in secondary hospitals, small clinics, or resource-limited settings. With the integration of a sample preparation module[38] and small operating gear, this sd-SlipChip can potentially be impactful for quantification of viral load in decentralized settings.

## RESULTS AND DISCUSSION

The sd-SlipChip consists of two opposing microfluidic plates that have microfabricated microwells and fluidic ducts on the contacting surface. The top plate contains one row of mother microwells and rows of fluidic ducts; the bottom plate contains one row of complementary mother microwells and rows of daughter microwells (Figure 1A). The size, volume, and number of microwells can be predetermined by requirements for specific applications, thus minimizing calculation or handling mistakes from operators. A lubricant (mineral oil: tetradecane at a 1:1 volumetric ratio) was placed in between the top layer and bottom layer to prevent the evaporation of droplets or the absorption of biomolecules to the surface of the microfluidic plate. The top and bottom plates were assembled to an initial position: the mother microwells on the top plate and their complementary parts on the bottom plate partially overlapped to establish a Type-I continuous fluidic path, which consists of mother microwells and complementary mother wells; the fluidic ducts on the top plate and the daughter microwells on the bottom plate partially overlapped to form Type-II continuous fluidic paths, which consists of daughter microwells (Figure 1B). A solution containing a high concentration of target molecules (Solution-I) was introduced into the Type-I fluidic path by pipetting, and a solution containing dilution buffer (Solution-II) was loaded into the Type-II fluidic paths (Figure 1C). Then, the top plate was slipped to the right relative to the bottom plate to disconnect all the fluidic paths and partition reagents (Figure 1D). To perform a dilution, the top plate was moved downward relative to the bottom plate to allow the mother microwells on the top plate to overlap with the first row of daughter microwells on the bottom plate, and the solution in the microwells was mixed by molecular diffusion (Figure 1E). Then, the top plate was slipped downward relative to the bottom plate again to allow the mother microwells on the top plate to break from the first row of daughter microwells and overlap with the second row of daughter microwells on the bottom plate (Figure 1F). Through the simple stepwise slipping movements between the top and bottom plate, a serial dilution nanoliter array was established (Figure 1G-I).

To ensure sufficient mass transfer during serial dilution, we first characterized the mixing between the mother microwells on the top plate and the daughter microwells on the bottom plate when they were brought into contact. An aqueous solution containing

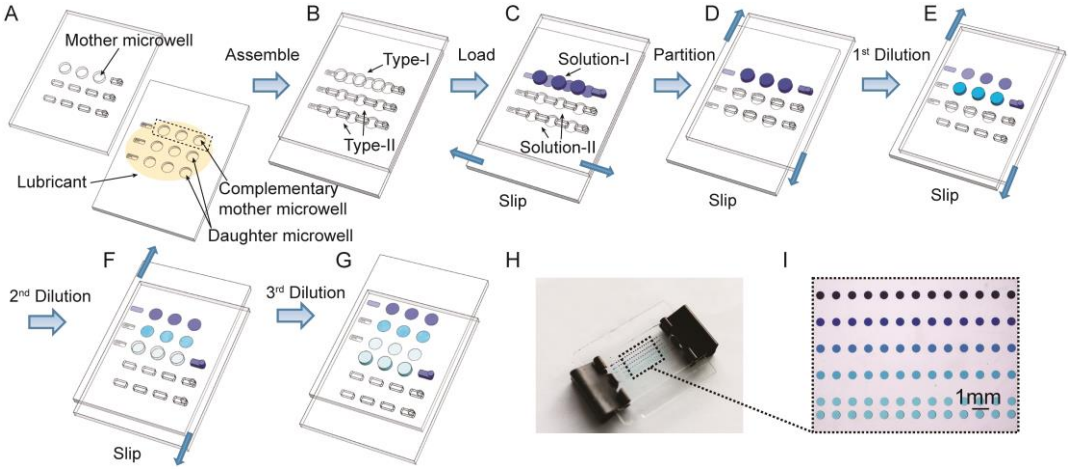


Figure 1. Schematic drawings for sd-SlipChip operations. A) The top and bottom plates of the sd-SlipChip device. B) Assembly of the sd-SlipChip by partially overlapping the wells and ducts on the contacting surface of two plates. C) Original solution (Solution-I) and dilution buffer (Solution-II) were introduced into Type-I and Type-II channels, respectively. D) The top plate moved right to form isolated reaction partitions. E) The top plate moved down to perform the 1st dilution step. F) The top plate moved down for the 2nd time to perform the 2nd dilution step. G) The top plate moved down for the 3rd time to separate the wells on the top layer from the wells on the bottom layer. H) A photo of a four-step sd-SlipChip. I) Zoomed-in photo shows the serial dilution pattern of blue dye.

fluorescein and, later, an aqueous solution containing DNA template were tested (see Methods in Supporting Information). The results suggested that 2 minutes of passive mixing by diffusion was sufficient to allow fluorescein and DNA template to reach an equilibrium concentration (Figure S1A-B). Therefore, a passive mixing time of 3 minutes was applied to the following serial dilution experiments.

Next, we demonstrated that the sd-SlipChip can achieve different mixing ratios with high accuracy. Devices containing 20 microwells per row were used. A dilution ratio of 1:1 was achieved by using an sd-SlipChip containing top wells of 10 nL and bottom wells of 10 nL. A dilution ratio of 1:2 was achieved by using an sd-SlipChip containing top wells of 5 nL and bottom wells of 10 nL. A dilution ratio of 1:4 was achieved by using an sd-SlipChip containing top wells of 3 nL and bottom wells of 12 nL. An aqueous solution containing 100 ng/ml fluorescein was introduced into the mother microwells, and water was loaded in the daughter microwells. The measured fluorescent intensity was in good agreement with the designed dilution ratio (Figure 2A-C).

We designed an eight-step sd-SlipChip with a fewer than 600 total wells to perform digital LAMP quantification over a large dynamic range of 7 orders of magnitude (Figure S2). This sd-SlipChip contains 8 rows of daughter microwells and 64 of 12 nL microwells per row for daughter microwells. This device contains 64 of 3 nL mother microwells and 64 of 12 nL complementary mother microwells. Based on the previous computational analysis of digital PCR by serial dilution,[39] as few as 50 partitions for digital nucleic acid analysis can obtain reasonably good sensitivity for copy number and assay sensitivity. The dilution factor for each step was 5. The calculated total dilution ratio was 390,625-fold. By preserving the high concentration sample stock in the 64 of 12 nL complimentary mother microwells (top row in Figure 3G) and utilizing all 8 rows of daughter microwells, the full dynamic range from the 9 rows can be expanded beyond the total dilution ratio. The theoretical upper limit of quantification (ULQ) was about $1.0\times10^8$ copies/μL, and the theoretical lower detection limit (LDL) was about 4 copies/μL. The dynamic range can be defined as ULQ/LDL,[34] therefore, this sd-SlipChip device can achieve a dynamic range of $2.5 \times 10^7$ fold, which is approximately 7 orders of magnitude.

We characterized the serial dilution digital LAMP on the sd-SlipChip by quantification of HBV plasmid DNA. The experimental setup is described in detail in the experimental section. Solution-I, containing LAMP mastermix, primers, bovine serum albumin (BSA), and HBV plasmid DNA template, was loaded into the mother microwells; Solution-II, containing LAMP master mix, primers, and BSA, was introduced into the daughter microwells. After multiple slipping operations, a nanoliter array of 64 complementary mother microwells (12 nL each) and $64 \times 8$ daughter microwells (12 nL each) was established. The device was placed on top of an in situ PCR thermal cycler for 30 minutes, and the resulting fluorescence signal was measured with a fluorescence microscope. None of the microwells in the no template control experiments showed a significant increase in fluorescence intensity (Figure 3A). At low concentrations of HBV DNA, only row one and row two presented digital patterns of positive wells (Figure 3B). As the concentration of target DNA increased, the 3rd to 8th dilutions demonstrated digital patterns (Figure 3C-G). The number of positive wells for each row was counted (Figure 3H). The calculated concentration from the experimental results (detailed calculation method in the Supporting Information) was in excellent agreement with the serial dilution ratio (Figure 3I).

We further tested serial dilution digital LAMP on an sd-SlipChip with HBV DNA extracted from clinical samples. Plasma samples from twelve anonymous HBV-positive patients and plasma samples from four anonymous HBV-negative patients were used in this study (experimental details in the Supporting Information). For the twelve HBV-positive samples, the quantification results from serial dilution digital LAMP on the sd-SlipChip were in good agreement with the results from standard HBV clinical protocols (Figure 3J). The four HBV-negative samples also tested negative on the sd-SlipChip as none of the microwells had fluorescent intensity higher than the cut-off threshold.

The sd-SlipChip can precisely control the dilution ratio by controlling the volumes of microwells. A fine gradient can be obtained by a small dilution ratio, and a large dynamic range can be the result of a large dilution ratio. The dilution ratio can also be different for different rows; for example, the dilution ratio increases as the number of rows increases to obtain a nonlinear serial dilution array. Furthermore, the dilution ratio

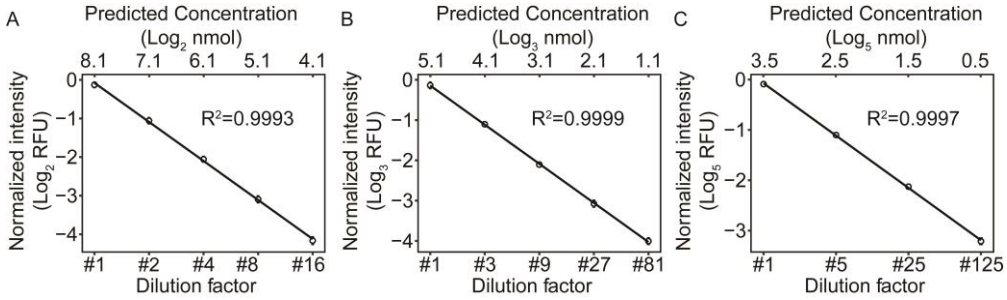


Figure 2. Characterization of the sd-SlipChip with different dilution ratios. An aqueous solution containing fluorescein was pipetted into the mother microwells, and water was loaded into the daughter microwells. A molecular diffusion time of 3 minutes was used for the following serial dilution experiments. The dilution ratio can be precisely predetermined by the volumes of mother microwells and daughter microwells. The x axis represents the dilution factor (log-transformed), and the y axis represents the normalized fluorescence intensity (log-transformed). A) Dilution ratio of 1:1. The volume ratio between mother and daughter microwells was 1:1. B) Dilution ratio of 1:2. The volume ratio between mother and daughter microwells was 1:2. C) Dilution ratio of 1:4. The volume ratio between mother and daughter microwells was 1:4. The error bar represents the standard deviation. (n=20).

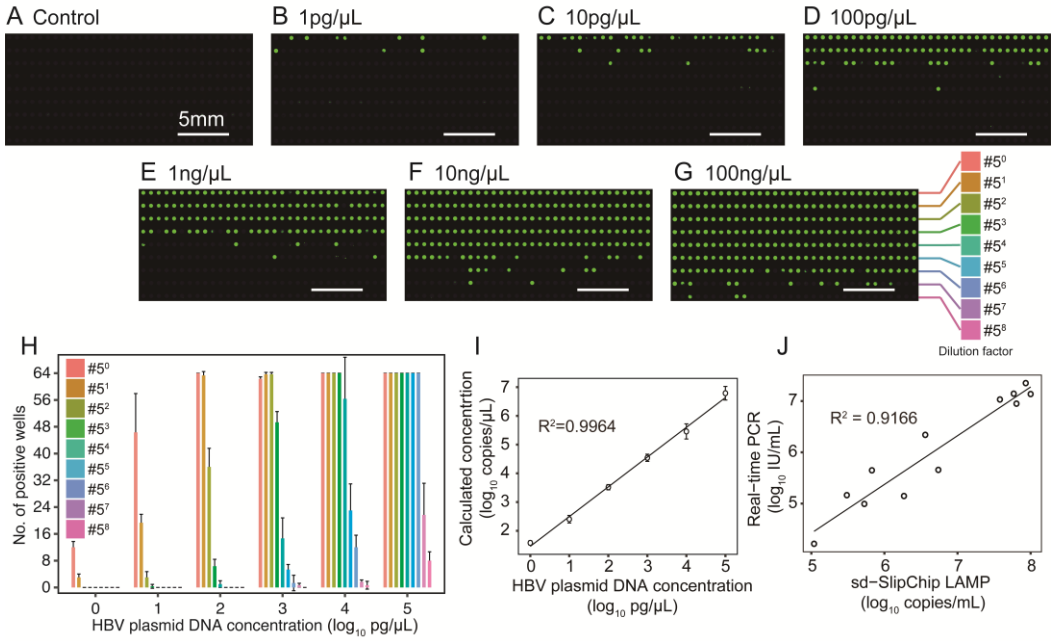


Figure 3. Large dynamic quantification of nucleic acid by digital LAMP on an eight-step sd-SlipChip with a dilution ratio of 1:4. (A-G) Representative fluorescence images of digital LAMP for quantification of HBV plasmid DNA. A) No template control. B) 1 pg/μL. C) 10 pg/μL. D) 100 pg/μL. E) 1 ng/μL. F) 10 ng/μL. G) 100 ng/μL. A green dot indicates a positive well. H) Bar chart representing the positive well count for each row at different concentrations for the quantification of HBV plasmid DNA (n=3). The different colors show different dilution factors, and the error bar represents the standard deviation. I) Plots of HBV plasmid DNA concentrations versus calculated concentrations from a linear regression for the quantification of HBV plasmid DNA. The x axis shows the HBV plasmid DNA concentration (log-transformed), and the y axis represents the copy number obtained by the sd-SlipChip method (log-transformed). J) HBV viral load with clinical samples comparing digital LAMP on an sd-SlipChip and a real-time PCR method. The x axis shows the copy number calculated by the sd-SlipChip method. The y axis represents the HBV viral load, which was quantified by real-time PCR.

per column can also be adjusted according to specific requirements to obtain multiple arrays of different serial dilution patterns on the same sd-SlipChip.

In this paper, the mixing of solution in mother microwells and daughter microwells simply relied on molecular diffusion. For systems with high diffusion coefficients, this may not be problematic. However, for more viscous solutions, systems with low diffusion coefficients, or systems requiring fast mixing, magnetic balls or micro stir bars can be placed in the mother microwells to perform active mixing.

Furthermore, analysis of paired data from the same column of an sd-SlipChip can provide an internal control and potentially increase the accuracy of analysis. In this paper, we took the base row, the first row that has more than 36.8% negative counts, and the rows below for data analysis. This method can use only the counts per row for calculation, but it does not fully utilize the paired relationship within each column. Further statistical tools or computational algorithms that perform additional analysis with data can provide more comprehensive results and additional insight on the error rate for the sd-SlipChip, but these approaches are beyond the scope of this paper.

## CONCLUSION

The sd-SlipChip can generate serial dilution nanoliter arrays with simple multistep slipping operations. It does not require cumbersome manual pipetting steps or complex fluidic handling systems. The sd-SlipChip can provide a precise dilution ratio by controlling the fluidic volumes in mother and daughter microwells. The sd-SlipChip can achieve analysis over a large dynamic range with significantly fewer reaction compartments than those produced with single-volume partitions. We applied the sd-SlipChip to digital LAMP quantification of target nucleic acids with a large dynamic range. The sd-SlipChip also has great potential for other biological or chemical screening applications over a large dynamic range, such as drug screening, immunoassays, protein crystallization, and optimization of reaction conditions.

## ASSOCIATED CONTENT

### Supporting Information

The following files are available free of charge:
methods, supporting figures and table, authors' contributions.

## AUTHOR INFORMATION

### Corresponding Author

ruth_limin@126.com; feng.shen@sjtu.edu.cn

## ACKNOWLEDGMENTS

This work is supported by the National Natural Science Foundation of China (No. 21705109), the Innovation Research Plan supported by the Shanghai Municipal Education Commission (No. ZXWF082101), and the Shanghai Jiao Tong University fund (No. WF220408214).

## REFERENCES


(1) McCallum, C. M.; Comai, L.; Greene, E. A.; Henikoff, S. Targeted Screening for Induced Mutations. *Nat. Biotechnol.* **2000**, *18*, 455.
(2) Emerson, J. F.; Ngo, G.; Emerson, S. S. Screening for Interference in Immunoassays. *Clin. Chem.* **2003**, *49* (7), 1163–1169.
(3) Scheler, O.; Pacocha, N.; Debski, P. R.; Ruszczak, A.; Kaminski, T. S.; Garstecki, P. Optimized Droplet Digital CFU Assay (DdCFU) Provides Precise Quantification of Bacteria over a Dynamic Range of 6logs and Beyond. *Lab Chip* **2017**, *17* (11), 1980–1987.
(4) Ben-David, A.; Davidson, C. E. Estimation Method for Serial Dilution Experiments. *J. Microbiol. Methods* **2014**, *107*, 214–221.
(5) Whitesides, G. M. The Origins and the Future of Microfluidics. *Nature* **2006**, *442* (7101), 368–373.
(6) Dertinger, S. K. W.; Chiu, D. T.; Noo Li Jeon; Whitesides, G. M. Generation of Gradients Having Complex Shapes Using Microfluidic Networks. *Anal. Chem.* **2001**, *73* (6), 1240–1246.
(7) Irimia, D.; Geba, D. A.; Toner, M. Universal Microfluidic Gradient Generator. *Anal. Chem.* **2006**, *78* (10), 3472–3477.
(8) Walker, G. M.; Monteiro-Riviere, N.; Rouse, J.; O'Neill, A. T. A Linear Dilution Microfluidic Device for Cytotoxicity Assays. *Lab Chip* **2007**, *7* (2), 226–232.
(9) Lee, K.; Kim, C.; Ahn, B.; Panchapakesan, R.; Full, A. R.; Nordee, L.; Kang, J. Y.; Oh, K. W. Generalized Serial Dilution Module for Monotonic and Arbitrary Microfluidic Gradient Generators. *Lab Chip* **2009**, *9* (5), 709–717.
(10) Sip, C. G.; Bhattacharjee, N.; Folch, A. A Modular Cell Culture Device for Generating Arrays of Gradients Using Stacked Microfluidic Flows. *Biomicrofluidics* **2011**, *5* (2).
(11) Sackmann, E. K.; Fulton, A. L.; Beebe, D. J. The Present and Future Role of Microfluidics in Biomedical Research. *Nature* **2014**, *507* (7491), 181–189.
(12) Ahrar, S.; Hwang, M.; Duncan, P. N.; Hui, E. E. Microfluidic Serial Dilution Ladder. *Analyst* **2014**, *139* (1), 187–190.
(13) Paegel, B. M.; Grover, W. H.; Skelley, A. M.; Mathies, R. A.; Joyce, G. F. Microfluidic Serial Dilution Circuit. *Anal. Chem.* **2006**, *78* (21), 7522–7527.
(14) Hattori, K.; Sugiura, S.; Kanamori, T. Generation of Arbitrary Monotonic Concentration Profiles by a Serial Dilution Microfluidic Network Composed of Microchannels with a High Fluidic-Resistance Ratio<. *Lab Chip* **2009**, *9* (12), 1763–1772.
(15) Kim, T. H.; Kim, C. J.; Kim, Y.; Cho, Y. K. Centrifugal Microfluidic System for a Fully Automated N-Fold Serial Dilution. *Sensors Actuators, B Chem.* **2018**, *256*, 310–317.
(16) Hindson, B. J.; Ness, K. D.; Masquelier, D. A.; Belgrader, P.; Heredia, N. J.; Makarewicz, A. J.; Bright, I. J.; Lucero, M. Y.; Hiddessen, A. L.; Legler, T. C.; Kitano, T. K.; Hodel, M. R.; Petersen, J. F.; Wyatt, P. W.; Steenblock, E. R.; Shah, P. H.; Bousse, L. J.; Troup, C. B.; Mellen, J. C.; Wittmann, D. K.; Erndt, N. G.; Cauley, T. H.; Koehler, R. T.; So, A. P.; Dube, S.; Rose, K. A.; Montesclaros, L.; Wang, S. L.; Stumbo, D. P.; Hodges, S. P.; Romine, S.; Milanovich, F. P.; White, H. E.; Regan, J. F.; Karlin-Neumann, G. A.; Hindson, C. M.; Saxonov, S.; Colston, B. W. High-Throughput Droplet Digital PCR System for Absolute Quantitation of DNA Copy Number. *Anal. Chem.* **2011**, *83* (22), 8604–8610.
(17) Mazutis, L.; Araghi, A. F.; Miller, O. J.; Baret, J.-C.; Frenz, L.; Janoshazi, A.; Taly, V.; Miller, B. J.; Hutchison, J. B.; Link, D.; Griffiths, A. D.; Rychelynck, M. Droplet-Based Microfluidic Systems for High-Throughput Single DNA Molecule Isothermal Amplification and Analysis. *Anal. Chem.* **2009**, *81* (12), 4813–4821.
(18) Lo, Y. M. D.; Lun, F. M. F.; Chan, K. C. A.; Tsui, N. B. Y.; Chong, K. C.; Lau, T. K.; Leung, T. Y.; Zee, B. C. Y.; Cantor, C. R.; Chiu, R. W. K. Digital PCR for the Molecular Detection of Fetal Chromosomal Aneuploidy. *PNAS* **2007**, *104* (32), 13116–13121.
(19) Huang, J. T.; Liu, Y. J.; Wang, J.; Xu, Z. G.; Yang, Y.; Shen, F.; Liu, X. H.; Zhou, X.; Liu, S. M. Next Generation Digital PCR Measurement of Hepatitis B Virus Copy Number in Formalin-Fixed Paraffin-Embedded Hepatocellular Carcinoma Tissue. *Clin. Chem.* **2015**, *61* (1), 290–296.
(20) Li, M.; Chen, W.; Papadopoulos, N.; Goodman, S. N.; Bjerregaard, N. C.; Laurberg, S.; Levin, B.; Juhl, H.; Arber, N.; Moinova, H.; Durkee, K.; Schmidt, K.; He, Y. P.; Diehl, F.; Velculescu, V. E.; Zhou, S. B.; Diaz, L. A.; Kinzler, K. W.; Markowitz, S. D.; Vogelstein, B. Sensitive Digital Quantification of DNA Methylation in Clinical Samples. *Nat. Biotechnol.* **2009**, *27*, 858.
(21) Taly, V.; Pekin, D.; Benhaim, L.; Kotsopoulos, S. K.; Corre, D. Le; Li, X.; Atochin, I.; Link, D. R.; Griffiths, A. D.; Pallier, K.; Blons, H. Bouche, O.; Landi, B.; Hutchison, J. B. Laurent-Puig, P. Multiplex Picodroplet Digital PCR to Detect KRAS Mutations in Circulating DNA from the Plasma of Colorectal Cancer Patients. *Clin. Chem.* **2013**, *59* (12), 1722–1731.
(22) Kiss, M. M.; Ortoleva-donnelly, L.; Beer, N. R.; Warner, J.; Bailey, C. G.; Colston, B. W.; Rothberg, J. M.; Link, D. R.; Leamon, H. High-Throughput Quantitative PCR in Picoliter Droplets Margaret. *Anal. Chem.* **2009**, *80* (23), 8975–8981.
(23) Cronier, S. A.; Mathies, R. A.; Blazej, R. G.; Kumaresan, P.; Yang, C. J. High-Throughput Single Copy DNA Amplification and Cell Analysis in Engineered Nanoliter Droplets. *Anal. Chem.* **2008**, *80* (10), 3522–3529.
(24) Hatch, A. C.; Fisher, J. S.; Tovar, A. R.; Hsieh, A. T.; Lin, R.; Pentoney, S. L.; Yang, D. L.; Lee, A. P. 1-Million Droplet Array with Wide-Field Fluorescence Imaging for Digital PCR. *Lab Chip* **2011**, *11* (22), 3838–3845.
(25) Xu, X.; Yuan, H.; Song, R.; Yu, M.; Chung, H. Y.; Hou, Y.; Shang, Y.; Zhou, H.; Yao, S. High Aspect Ratio Induced Spontaneous Generation of Monodisperse Picolitre Droplets for Digital PCR. *Biomicrofluidics* **2018**, *12* (1), 1–10.
(26) Ottesen, E. A.; Hong, J. W.; Quake, S. R.; Leadbetter, J. R. Environmental Bacteria. *Science (80-. ).* **2006**, No. 314, 1464–1467.
(27) Wang, J.; Kreutz, J. E.; Thompson, A. M.; Qin, Y.; Sheen, A. M.; Wang, J.; Wu, L.; Xu, S.; Chang, M.; Raugi, D. N.; Smith, R. A.; Gottlieb, G. S.; Chiu, D. T. SD-Chip Enabled Quantitative Detection of HIV RNA Using Digital Nucleic Acid Sequence-Based Amplification (DNASBA). *Lab Chip* **2018**, *18* (22), 3501–3506.
(28) Gou, T.; Hu, J.; Wu, W.; Ding, X.; Zhou, S.; Fang, W.; Mu, Y. Smartphone-Based Mobile Digital PCR Device for DNA Quantitative Analysis with High Accuracy. *Biosens. Bioelectron.* **2018**, *120* (May), 144–152.
(29) Heyries, K. A.; Tropini, C.; VanInsberghe, M.; Doolin, C.; Petriv, O. I.; Singhal, A.; Leung, K.; Hughesman, C. B.; Hansen, C. L. Megapixel Digital PCR. *Nat. Methods* **2011**, *8*, 649.
(30) Men, Y.; Fu, Y.; Chen, Z.; Sims, P. A.; Greenleaf, W. J.; Huang, Y. Digital Polymerase Chain Reaction in an Array of Femtoliter Polydimethylsiloxane Microreactors. *Anal. Chem.* **2012**, *84* (10), 4262–4266.
(31) Shen, F.; Du, W.; Kreutz, J. E.; Fok, A.; Ismagilov, R. F. Digital PCR on a SlipChip. *Lab Chip* **2010**, *10* (20), 2666–2672.
(32) Shen, F.; Davydova, E. K.; Du, W.; Kreutz, J. E.; Piepenburg, O.; Ismagilov, R. F. Digital Isothermal Quantification of Nucleic Acids via Simultaneous Chemical Initiation of Recombinase Polymerase Amplification Reactions on SlipChip. *Anal. Chem.* **2011**, *83* (9), 3533–3540.
(33) Shen, F.; Sun, B.; Kreutz, J. E.; Davydova, E. K.; Du, W.; Reddy, P. L.; Joseph, L. J.; Ismagilov, R. F. Multiplexed Quantification of Nucleic Acids with Large Dynamic Range Using Multivolume Digital RT-PCR on a Rotational SlipChip Tested with HIV and Hepatitis C Viral Load. *J. Am. Chem. Soc.* **2011**, *133* (44), 17705–17712.
(34) Kreutz, J. E.; Munson, T.; Huynh, T.; Shen, F.; Du, W.; Ismagilov, R. F. Theoretical Design and Analysis of Multivolume Digital Assays with Wide Dynamic Range Validated Experimentally with Microfluidic Digital PCR. *Anal. Chem.* **2011**, *83* (21), 8158–8168.
(35) Abe, A. K. I.; Inoue, K.; Tanaka, T.; Kato, J.; Kajiyama, N.; Kawaguchi, R.; Tanaka, S.; Yoshiba, M.; Kohara, M.; Icrobiol, J. C. L. I. N. M. Quantitation of Hepatitis B Virus Genomic DNA by Real-Time Detection PCR. *J. Clin. Microbiol.* **1999**, *37* (9), 2899–2903.
(36) Gra, P. E.; Peyton, C.; Wheeler, C.; Apple, R.; Higuchi, R.; Shah, K. V. Reproducibility of HPV 16 and HPV 18 v Iral Load Quantitation Using TaqMan Real-Time PCR Assays. *J. Virol. Methods* **2003**, *112*, 23–33.
(37) Saag, M. S.; Holodniy, M.; Kuritzkes, D. R.; O'Brien, W. A.; Coombs, R.; Poscher, M. E.; Jacobsen, D. M.; Shaw, G. M.; Richman, D. D.; Volberding, P. A. HIV Viral Load Markers in Clinical Practice. *Nat. Med.* **1996**, *2*, 625.
(38) Schlappi, T. S.; McCalla, S. E.; Schoepp, N. G.; Ismagilov, R. F. Flow-through Capture and in Situ Amplification Can Enable Rapid Detection of a Few Single Molecules of Nucleic Acids from Several Milliliters of Solution. *Anal. Chem.* **2016**, *88* (15), 7647–7653.
(39) Deng, X.; Custer, B. S.; Busch, M. P.; Bakkour, S.; Lee, T. H. Simultaneous Estimation of Detection Sensitivity and Absolute Copy Number from Digital PCR Serial Dilution. *Comput. Biol. Chem.* **2017**, *68*, 1–5.

Table of contents graphic